

ENCLOSURE 1

APP-GW-GLR-026

Revision 2

“New Fuel Storage Rack Structural/Seismic Analysis”

Technical Report Number 44

November 2009

# **AP1000 Standard Combined License Technical Report**

## **New Fuel Storage Rack Structural/Seismic Analysis**

---

Westinghouse Electric Company LLC  
P.O. Box 355  
Pittsburgh, PA 15230-0355

© 2009 Westinghouse Electric Company LLC  
All Rights Reserved

**TABLE OF CONTENTS**

LIST OF TABLES .....	4
LIST OF FIGURES .....	5
1 INTRODUCTION .....	6
2 TECHNICAL BACKGROUND .....	7
2.1 DESIGN .....	7
2.1.1 AP1000 New Fuel Storage Rack and Vault Description .....	7
2.2 METHODOLOGY .....	8
2.2.1 Acceleration Time Histories .....	8
2.2.2 Modeling Methodology .....	8
2.2.3 Simulation and Solution Methodology .....	11
2.2.4 Conservatisms Inherent in Methodology .....	12
2.3 KINEMATIC AND STRESS ACCEPTANCE CRITERIA .....	12
2.3.1 Introduction .....	12
2.3.2 Kinematic Criteria .....	12
2.3.3 Stress Limit Criteria .....	12
2.3.4 Stress Limits for Various Conditions Per ASME Code .....	13
2.3.5 Dimensionless Stress Factors .....	16
2.4 ASSUMPTIONS .....	16
2.5 INPUT DATA .....	17
2.5.1 Rack Data .....	17
2.5.2 Structural Damping .....	17
2.5.3 Material Data .....	17
2.6 COMPUTER CODES .....	17
2.7 ANALYSES .....	17
2.7.1 Acceptance Criteria .....	17
2.7.2 Dynamic Simulations .....	17
2.8 RESULTS OF ANALYSES .....	17
2.8.1 Time History Simulation Results .....	18
2.8.2 Rack Structural Evaluation .....	19
2.8.3 Dead Load Evaluation .....	21
2.8.4 Local Stress Considerations .....	22
2.8.5 Hypothetical Fuel Assembly Drop Accidents .....	22
2.8.6 Stuck Fuel Assembly Evaluation .....	23
2.9 CONCLUSIONS .....	23
3 REGULATORY IMPACT .....	44
4 REFERENCES .....	45
5 DCD MARKUP .....	47

**LIST OF TABLES**

Table 2-1	AP1000 New Fuel Storage Rack Storage Cell Description .....	25
Table 2-2	Simulation Listing.....	25
Table 2-3	Loading Combinations for AP1000 New Fuel Storage Rack .....	26
Table 2-4	AP1000 New Fuel Storage Rack and Fuel Data .....	27
Table 2-5	Material Data (ASME - Section II, Part D) .....	28
Table 2-6	Results Summary .....	28
Table 2-7	Time History Post-Processor Results.....	28
Table 2-8	Rack-to-Wall Impacts .....	28
Table 2-9	Maximum Stress Factors.....	29
Table 2-10	Baseplate-to-Rack Maximum Weld Stress.....	29
Table 2-11	Base Metal Shear Stress.....	29
Table 2-12	Baseplate-to-Pedestal Welds .....	29
Table 2-13	Weld and Base Metal Shear Results .....	30
Table 2-14	Pedestal Thread Shear Stress .....	30
Table 2-15	Computer Codes Used for AP1000 New Fuel Storage Rack Structural/Seismic Analysis .....	31
Table 2-16	Degrees of Freedom for Single Rack Dynamic Model.....	32
Table 2-17	Results from Stuck Fuel Assembly Evaluation.....	32

**LIST OF FIGURES**

Figure 2-1	Configuration of New Fuel Storage Rack (Sheet 1 of 2).....	33
Figure 2-1	Configuration of New Fuel Storage Rack (Sheet 2 of 2).....	34
Figure 2-2	Schematic Diagram of Dynamic Model for DYNARACK .....	35
Figure 2-3	Rack-to-Rack Impact Springs.....	36
Figure 2-4	Fuel-to-Rack Impact Springs at Level of Rattling Mass.....	37
Figure 2-5	Two-Dimensional View of Spring-Mass Simulation .....	38
Figure 2-6	Rack Degrees-of-Freedom for X-Y Plane Bending with Shear and Bending Spring .....	39
Figure 2-7	LS-DYNA Model of Dropped Fuel Assembly.....	40
Figure 2-8	LS-DYNA Model of Top and Bottom of AP1000 New Fuel Storage Rack.....	41
Figure 2-9	Results from Drop on AP1000 New Fuel Storage Rack .....	42
Figure 2-10	Baseplate Deformation Resulting from Fuel Assembly Drop onto Baseplate .....	43

# 1 INTRODUCTION

This report summarizes the structural/seismic analysis of the AP1000 New Fuel Storage Rack. Revision one specifically addresses three items: changes to the design; reanalysis of the new fuel rack for the envelope of hard rock and soil conditions as documented in Reference 24; and supplemental information added as a result of NRC Requests for Additional Information. Revision two incorporates finalized responses to additional NRC RAIs.

The AP1000 New Fuel Storage Rack is used to temporarily store fresh fuel assemblies until they are loaded into the reactor core. The requirements for this analysis are identified in the AP1000 Design Control Document (DCD), subsection 9.1.1.2.1 (Reference 1). The completion of this analysis is identified as Combined Operating License (COL) Information Item 9.1-1 (Final Safety Evaluation Report [Reference 2] Action Item 9.1.6-1) in DCD subsection 9.1.6 to be completed by the Combined License applicant.

COL Information Item 9.1-1: "Perform a confirmatory structural dynamic and stress analysis for the new fuel rack, as described in AP1000 DCD subsection 9.1.1.2.1."

This COLA technical report closes this COL information item. The calculations "AP1000 New Fuel Storage Rack Structural/Seismic Analysis" (Reference 3) and "Analyses of AP1000 Fuel Storage Racks Subjected to Fuel Drop Accidents" (Reference 28) are available for U. S. Nuclear Regulatory Commission (NRC) audit. A summary of the criticality analysis for the AP1000 New Fuel Storage Rack is presented in AP1000 Standard Combined License Technical Report, "New Fuel Storage Rack Criticality Analysis" (Reference 4).

Per DCD subsection 3.7.5.2, Combined License applicants will prepare site-specific procedures for activities following an earthquake. These procedures will be used to accurately determine both the response spectrum and cumulative absolute velocity of the recorded earthquake ground motion from the seismic instrumentation system. An activity will be to address measurement of the post-seismic event gaps between the new fuel rack and walls of the new fuel storage pit and to take appropriate corrective actions.

## 2 TECHNICAL BACKGROUND

This report considers the structural adequacy of the proposed AP1000 New Fuel Storage Rack under postulated loading conditions. Analyses and evaluations follow the NRC Standard Review Plan 3.8.4, Revision 1 (Reference 6). Although the licensing basis for the AP1000 design invokes NRC SRP 3.8.4, Revision 1, an evaluation has been performed to confirm that the stress analysis of the new fuel rack also satisfies the applicable provisions of NRC SRP 3.8.4, Revision 2 (Reference 25). The dynamic analyses use a time-history simulation code used in numerous previous fuel rack licensing efforts in the United States and abroad. This report provides a discussion of the method of analyses, modeling assumptions, key evaluations, and results obtained to establish the margins of safety. The objective of this report is to develop the loads on the AP1000 New Fuel Storage Rack and confirm that the loads do not pose a threat to the stored fuel assemblies.

### 2.1 DESIGN

#### 2.1.1 AP1000 New Fuel Storage Rack and Vault Description

The configuration of the AP1000 New Fuel Storage Rack is shown in Figure 2-1 and an overview of the construction and materials used in the AP1000 New Fuel Storage Rack is presented in Table 2-1.

The AP1000 New Fuel Storage Rack is freestanding and sits inside a concrete room (vault) in the Auxiliary Building. It consists of a 8x9 array of storage cells, which provides 72 total storage locations. A vault lid is provided for security, and for Foreign Material Exclusion (FME).

The individual storage cells of the AP1000 New Fuel Storage Rack are centered on a nominal pitch of 10.9 inches. Each storage cell consists of an inner stainless steel box, which has a nominal inside dimension of 8.8 inches and is 0.075 inches thick. Metamic<sup>®</sup> poison panels are attached to the outside surfaces of all storage cells except for the outside cell walls directly facing the north and south walls of the vault. No poison panels are required on these outside cell faces since there is only a small amount of space between the rack and storage vault concrete. However, poison panels are placed on the outside cell faces in the east and west directions (see Figure 2-1) to mitigate the effects of an inadvertent placement of a fuel assembly outside of the rack, but within the vault on these two sides if the vault lid is ever removed. Each Metamic poison panel is held in place and is centered on the surface of the stainless steel box by an outer stainless steel sheathing panel. There is a small void space between the sheathing and the Metamic panel. The Metamic poison panels are 7.5 inches wide by 0.106 inches thick. The sheathing panels are 0.035 inches thick.

Each storage cell is nominally 199.5 inches long, and it rests on top of a base plate whose top is 5 inches above the new fuel vault floor. Note that each Metamic poison panel is 172 inches long, overlapping the 168-inch active fuel length. The Metamic poison material is a mixture of B<sub>4</sub>C, nominally 31.0 weight-percent, and aluminum, 69.0 weight-percent.

## 2.2 METHODOLOGY

### 2.2.1 Acceleration Time Histories

The response of a freestanding rack module to seismic inputs is highly nonlinear, and it involves a complex combination of motions (sliding, rocking, twisting, and turning), resulting in impacts and frictional effects. Linear methods, such as modal analysis and response spectrum techniques, cannot accurately replicate the response of such a highly nonlinear structure to seismic excitation. An accurate simulation is obtained only by direct integration of the nonlinear equations of motion using actual pool slab acceleration time-histories as the forcing function. Therefore, the initial step in AP1000 New Fuel Storage Rack qualification is to develop synthetic time-histories for three orthogonal directions that comply with the guidelines of the NRC Standard Review Plan 3.7.1, Revision 2 (Reference 7). The synthetic time-histories must meet the criteria of statistical independence, envelope the target design response spectra, and envelope the target Power Spectral Density function associated with the target response spectra.

The acceleration time histories for the New Fuel Floor Response Spectra (FRS) are used as the input motion for the seismic analysis of the new fuel rack. Three orthogonal components are input and solved simultaneously together with a constant 1-g gravity acceleration.

### 2.2.2 Modeling Methodology

#### 2.2.2.1 General Considerations

Once a set of input excitations is obtained, a dynamic representation is developed. Reliable assessment of the stress field and kinematic behavior of a rack module calls for a conservative dynamic model incorporating all key attributes of the actual structure. This means that the dynamic model must have the ability to execute concurrent bending, twisting, and other motion forms compatible with the free-standing installation of the module. Additionally, the model must possess the capability to effect momentum transfers that occur due to rattling of fuel assemblies inside storage cells. Since the AP1000 New Fuel Storage Rack is not placed in water, there is no contribution from water mass in the interstitial spaces around the rack module and within the storage cells. Finally, Coulomb friction coefficients at the pedestal to platform surface interfaces may lie in a rather wide range, depending on the design of those interfaces, and the model must be able to reflect their effect. In short, there are a large number of parameters with potential influence on the rack motion. A comprehensive structural evaluation must be able to incorporate all of these effects, in a finite number of analyses, without sacrificing conservatism.

The three-dimensional (3-D) dynamic model of a single fuel rack was introduced by Holtec International in 1980 and has been used in many re-rack projects since that time. These re-rack projects include Turkey Point, St. Lucie, and Diablo Canyon. The details of this classical methodology are presented in Reference 9. The 3-D model of a typical rack handles the array of variables as follows:

- Interface Coefficient of Friction

Coefficient of friction (COF) values are assigned at each interface, which reflect the realities of stainless steel-to-stainless steel contact. The mean value of coefficient of friction is 0.5, and the

limiting values are based on experimental data, which are bounded by the values 0.2 and 0.8 (Reference 20).

Although the seismic analysis of the AP1000 New Fuel Storage Rack considers three different coefficients of friction (0.2, 0.5, and 0.8 - the same conditions considered under wet conditions in the analysis of the AP1000 Spent Fuel Storage Racks) between the support pedestals and the pit liner, the reality is that the coefficient of friction will be greater than 0.5 since the new fuel pit, unlike the spent fuel pool, is not flooded with water. Per Reference 29, the static coefficient of friction for steel on steel (dry) is between 0.74 and 0.78; therefore only the results from the 0.5 and 0.8 coefficient of friction cases are considered credible. The results of the 0.2 coefficient of friction case are maintained in this report for continuity.

- **Impact Phenomena**

Compression-only spring elements, with gap capability, are used to provide for opening and closing of interfaces, such as the pedestal-to-bearing pad interface and fuel assembly-to-cell wall interface potential contact locations.

- **Fuel Loading Scenarios**

The dynamic analyses performed for the AP1000 New Fuel Storage Rack assume that all fuel assemblies within the rack rattle in unison throughout the seismic event, which obviously exaggerates the contribution of impact against the cell wall. An attenuation factor can be used to adjust for the random component of fuel assembly rattling. However, in this analysis, the attenuation factor equals one for all simulations (that is, fuel assemblies conservatively move perfectly in-phase).

- **Fluid Coupling**

Since the AP1000 New Fuel Storage Rack is installed in a dry enclosure, no fluid coupling effects are modeled in the dynamic simulations.

#### **2.2.2.2 Specific Modeling Details for a Single Rack**

The rack analysis is performed using a 3-D multi-degree of freedom model. For the dynamic analysis, the rack, plus contained rattling fuel, is modeled as a 22 Degree of Freedom (DOF) system. The rack cellular structure elasticity is modeled by a 3-D beam having 12 DOF (three translation and three rotational DOF at each end so that two-plane bending, tension/compression, and twist of the rack are accommodated). An additional two horizontal DOFs are ascribed to each of five rattling fuel masses, which are located at heights 0H, 0.25H, 0.5H, 0.75H, and H, where H is the height of a storage cell above the baseplate. While the horizontal motion of the rattling fuel mass is associated with five separate masses, the totality of the fuel mass is associated with the vertical motion and it is assumed that there is no fuel rattling in the vertical direction. In other words, the vertical displacement of the fuel is coupled with the vertical displacement of the rack (that is, degree of freedom "P3" in Figure 2-2) by lumping the entire stored fuel mass (in the vertical direction only) with the vertical rack mass at the baseplate level.

The beam model for the rack is assumed supported, at the base level, on four pedestals modeled with non-linear elements; these elements are properly located with respect to the centerline of the rack beam, and allow for arbitrary rocking and sliding motions. The horizontal rattling fuel masses transfer load to the new fuel rack through compression-only gap spring elements, oriented to allow impacts of each of the five rattling fuel masses with the rack cell in either or both horizontal directions at any instant in time. Figure 2-2 illustrates the typical dynamic rack model with the degrees of freedom shown for both the AP1000 New Fuel Storage Rack and for the rattling fuel mass. Table 2-16 defines the nodal DOFs for the dynamic model of a single rack as depicted in Figure 2-2. In order to simulate this behavior, the stored fuel mass is distributed among the five lumped mass nodes, for the rack, as follows:

	% of total stored fuel mass
• Top of rack (Node 2)	12.5%
• 3/4 height (Node 3)	25%
• 1/2 height (Node 4)	25%
• 1/4 height (Node 5)	25%
• Bottom of rack (Node 1)	12.5%

(See Figure 2-2.)

The stiffness of pedestal springs that simulate rack pedestal to the floor compression-only contact is modeled using contact and friction elements at the locations of the pedestals between pedestal and floor. Four contact springs (one at each corner location) and eight friction elements (two per pedestal) are included in each 22 DOF rack model.

Also shown in Figure 2-2 is a detail of the model of a typical support with a vertical compression-only gap element and two orthogonal elements modeling frictional behavior. These friction elements resist lateral loads, at each instant in time, up to a limiting value set by the current value of the normal force times the coefficient of friction. Figures 2-3 through 2-5 show schematic diagrams of the various (linear and non-linear) elements that are used in the dynamic model of a typical new fuel rack. Figure 2-3 shows the location of the compression-only gap elements that are used to simulate the rack-to-wall contact at every instant in time. Figure 2-4 shows the four compression-only gap elements at each rattling mass location, which serve to simulate rack-to-fuel assembly impact in any orientation at each instant in time. Figure 2-5 shows a two-dimensional elevation schematic depicting the five fuel masses and their associated gap/impact elements, the typical pedestal friction and gap impact elements. This figure combines many of the features shown in Figures 2-3 and 2-4, and it provides an overall illustration of the dynamic model used for the AP1000 New Fuel Storage Rack.

Finally, Figure 2-6 provides a schematic diagram of the coordinates and the beam springs used to simulate the elastic bending behavior and shear deformation of the rack cellular structure in two-plane bending. Not shown are the linear springs modeling the extension, compression, and twisting behavior of the cellular structure.

### Mass Matrix

Since there is no water in the AP1000 New Fuel Storage Rack enclosure, the mass matrix involves only the structural masses associated with the dynamic model.

## Stiffness Matrix

The spring stiffnesses associated with the elastic elements that model the behavior of the assemblage of cells within a rack are based on the representation developed in Reference 10. Tension-compression behavior and twisting behavior are each modeled by a single spring with linear or angular extension involving the appropriate coordinates at each end of the rack beam model. For simulation of the beam bending stiffness, a model is used consistent with the techniques of the reference based on a bending spring and a shear spring for each plane of bending, which connects the degrees of freedom associated with beam bending at each end of the rack. Impact and friction behavior is included using the piecewise linear formulations similarly taken from the reference.

The AP1000 New Fuel Storage Rack is subject to the New Fuel Floor Response Spectra for the AP1000 New Fuel Storage Rack (Reference 18). This is the combination of floor response spectra nodes closest to the floor of the new fuel storage vault located at 118' 2.5". The procedure used is consistent with the seismic analysis methods described in Section 3.7 of the DCD (Reference 1). Four runs are performed to bound possible coefficient of friction values and are summarized in Table 2-2.

### 2.2.3 Simulation and Solution Methodology

Recognizing that the analytical work effort must deal with both stress and displacement criteria, the sequence of model development and analysis steps that are undertaken for each simulation are summarized in the following:

- a. Prepare a 3-D dynamic model of the AP1000 New Fuel Storage Rack module.
- b. Archive for post-processing appropriate displacement and load outputs from the dynamic model.
- c. Perform stress analysis of high stress areas for rack dynamic runs. Demonstrate compliance with American Society for Mechanical Engineers (ASME) Code Section III, subsection NF (Reference 11) limits on stress and displacement. The high stress areas are associated with the pedestal-to-baseplate connection. In addition, some local evaluations are performed for the bounding case to ensure that the fuel remains protected under all impact loads.

For the transient analyses performed, a step-by-step solution in time uses a central difference algorithm. The solver computer algorithm, implemented in the Holtec Proprietary Code MR216 (a.k.a. DYNARACK), is given in Reference 10, and the documentation of MR216 is presented in Reference 12.

Using the 22-DOF rack structural model in each DYNARACK simulation, equations of motion corresponding to each degree-of-freedom are obtained using Lagrange's formulation of the dynamic equations of motion (Reference 10). The system kinetic energy includes contributions from the structural masses defined by the 22-DOF model.

Results are archived at appropriate time intervals for permanent record and for subsequent post-processing for structural integrity evaluations as follows:

- All generalized nodal displacement coordinate values in order to later determine the motion of the rack
- All load values for linear springs representing beam elasticity
- All load values for compression-only gap springs representing pedestals, rack-to-fuel impact, and rack-to-wall impacts
- All load values for friction springs at the pedestal/platform interface

#### **2.2.4 Conservatism Inherent in Methodology**

The following items are built-in conservatisms:

- All fuel rattling mass at each level is assumed to move as a unit thus maximizing impact force and rack response.
- Spring rates are computed in a conservative manner to use maximum values in the analysis. This tends to conservatively overestimate peak impact forces.
- Although not considered credible, the results from the 0.2 coefficient of friction case have been maintained and were carried through the evaluations when they were the most limiting case.

### **2.3 KINEMATIC AND STRESS ACCEPTANCE CRITERIA**

#### **2.3.1 Introduction**

The AP1000 New Fuel Storage Rack is designed as seismic Category I. The NRC Standard Review Plan 3.8.4 (Reference 6) states that the ASME Code Section III, subsection NF (Reference 11), as applicable for Class 3 Components, is an appropriate vehicle for design. The stress analysis of the new fuel rack also satisfies all of the applicable provisions in NRC Regulatory Guide 1.124, Revision 1 (Reference 26) for components designed by the linear elastic analysis method. In addition, an evaluation has been performed to confirm that the stress analysis of the new fuel rack also satisfies the applicable provisions of NRC Regulatory Guide 1.124, Revision 2 (Reference 27). In the following sections, the ASME limits are set down first, followed by any modifications by project specification, where applicable.

#### **2.3.2 Kinematic Criteria**

The AP1000 New Fuel Storage Rack should not exhibit rotations to cause the rack to overturn (in the east-west direction) (that is, ensure that the rack does not slide off the bearing pads, or exhibit a rotation sufficient to bring the center of mass over the corner pedestal).

#### **2.3.3 Stress Limit Criteria**

For thoroughness, the Standard Review Plan (Reference 6) load combinations were used. Stress limits must not be exceeded under the required load combinations. The loading combinations shown in

Table 2-3 are applicable for freestanding racks that are steel structures. (Note that there is no operating basis earthquake [OBE] event defined for the AP1000; therefore, loading conditions associated with an OBE event are not considered.)

### 2.3.4 Stress Limits for Various Conditions Per ASME Code

Stress limits for Normal Conditions are derived from the ASME Code, Section III, Subsection NF. Parameters and terminology are in accordance with the ASME Code. The AP1000 New Fuel Storage Rack is freestanding; thus, there is minimal or no restraint against free thermal expansion at the base of the rack. Moreover, thermal stresses are secondary, which strictly speaking, have no stipulated stress limits in Class 3 structures or components when acting in concert with seismic loadings. Thermal loads applied to the rack are, therefore, not included in the stress combinations involving seismic loadings.

Material properties for analysis and stress evaluation are provided in Table 2-5.

#### 2.3.4.1 Normal Conditions (Level A)

Normal conditions are as follows:

- Tension

Allowable stress in tension on a net section is:

$$F_t = 0.6 S_y$$

where  $S_y$  is the material yield strength at temperature. ( $F_t$  is equivalent to primary membrane stress.)

- Shear

Allowable stress in shear on a net section is:

$$F_v = 0.4 S_y$$

- Compression

Allowable stress in compression ( $F_a$ ) on a net section of Austenitic material is:

$$F_a = S_y(.47 - kl/444r)$$

where  $kl/r < 120$  for all sections and

$l =$  unsupported length of component.

- k = length coefficient which gives influence of boundary conditions, e.g.
- k = 1 (simple support both ends)
  - k = 2 (cantilever beam)
  - k = 0.5 (clamped at both ends)

Note: Evaluations conservatively use k = 2 for all conditions.

E = Young's modulus

r = radius of gyration of component = c/2.45 for a thin wall box section of mean side width c.

- Bending

Allowable bending stress ( $F_b$ ) at the outermost fiber of a net section due to flexure about one plane of symmetry is:

$$F_b = 0.60 S_y$$

- Combined Bending and Compression

Combined bending and compression on a net section satisfies:

$$f_a/F_a + C_{mx}f_{bx}/D_xF_{bx} + C_{my}f_{by}/D_yF_{by} < 1.0$$

where:

- $f_a$  = Direct compressive stress in the section
- $f_{bx}$  = Maximum bending stress for bending about x-axis
- $f_{by}$  = Maximum bending stress for bending about y-axis
- $C_{mx}$  = 0.85
- $C_{my}$  = 0.85
- $D_x$  =  $1 - (f_a/F'_{cx})$
- $D_y$  =  $1 - (f_a/F'_{cy})$
- $F'_{ex,ey}$  =  $(\pi^2 E)/(2.15 (kl/r)_{x,y}^2)$

and subscripts x and y reflect the particular bending plane.

- Combined Flexure and Axial Loads

Combined flexure and tension/compression on a net section satisfies:

$$(f_a/0.6 S_y) + (f_{bx}/F_{bx}) + (f_{by}/F_{by}) < 1.0$$

- Welds

Allowable maximum shear stress ( $F_w$ ) on the net section of a weld is:

$$F_w = 0.3 S_u$$

where  $S_u$  is the material ultimate strength at temperature. For the area in contact with the base metal, the shear stress on the gross section is limited to  $0.4S_y$ .

### 2.3.4.2 Upset Conditions (Level B)

Although the ASME Code allows an increase in allowables above those appropriate for normal conditions, any evaluations performed herein conservatively use the normal condition allowables.

### 2.3.4.3 Faulted (Abnormal) Conditions (Level D)

Section F-1334 (ASME Section III, Appendix F [Reference 14]), states that limits for the Level D condition are the smaller of 2 or  $1.167S_u/S_y$  times the corresponding limits for the Level A condition if  $S_u > 1.2S_y$ , or 1.4 if  $S_u \leq 1.2S_y$ , except for requirements specifically listed below.  $S_u$  and  $S_y$  are the properties of 304 stainless steel at the specified rack design temperature. Examination of material properties for 304 stainless steel demonstrates that 1.2 times the yield strength is less than the ultimate strength. Since  $1.167 * (75,000/30,000) = 2.92$ , the multiplier of 2.0 controls.

Exceptions to the above general multiplier are the following:

- Stresses in shear in the base metal shall not exceed the lesser of  $0.72S_y$  or  $0.42S_u$ . In the case of the austenitic stainless material used here,  $0.72S_y$  governs.
- Axial compression loads shall be limited to  $2/3$  of the calculated buckling load.
- Combined Axial Compression and Bending - The equations for Level A conditions shall apply except that:

$$F_a = 0.667 \times \text{Buckling Load/Gross Section Area,}$$

and  $F_{ex,ey}$  may be increased by the factor 1.65.

- For welds, the Level D allowable maximum weld stress is not specified in Appendix F of the ASME Code. An appropriate limit for weld throat is conservatively set here as:

$$F_w = (0.3 S_u) \times \text{factor}$$

where: factor = (Level D shear stress limit)/(Level A shear stress limit) =  $0.72 \times S_y / 0.4 \times S_y = 1.8$

therefore;  $F_w = (0.3 S_u) \times (1.8) = 0.54 S_u$

### 2.3.5 Dimensionless Stress Factors

In accordance with the methodology of the ASME Code, Section NF, where both individual and combined stresses must remain below certain values, the stress results are presented in dimensionless form. Dimensionless stress factors are defined as the ratio of the actual developed stress to the specified limiting value. The limiting value of each stress factor is 1.0 based on an evaluation that uses the allowable strength appropriate to Level A or Level D loading as discussed above.

- $R_1$  = Ratio of direct tensile or compressive stress on a net section to its allowable value (note pedestals only resist compression)
- $R_2$  = Ratio of gross shear on a net section in the x-direction to its allowable value
- $R_3$  = Ratio of maximum bending stress due to bending about the x-axis to its allowable value for the section
- $R_4$  = Ratio of maximum bending stress due to bending about the y-axis to its allowable value for the section
- $R_5$  = Combined flexure and compression factor (as defined in subsection 2.3.4.1)
- $R_6$  = Combined flexure and tension (or compression) factor (as defined in subsection 2.3.4.1)
- $R_7$  = Ratio of gross shear on a net section in the y-direction to its allowable value

At any location where stress factors are reported, the actual stress at that location may be recovered by multiplying the reported stress factor  $R$  by the allowable stress for that quantity. For example, if a reported Level A combined tension and two plane bending stress factor is  $R_6 = 0.85$ , and the allowable strength value is  $0.6S_y$ , then the actual combined stress at that location is  $\text{Stress} = R_6 \times (0.6S_y) = 0.51S_y$ .

### 2.4 ASSUMPTIONS

The following assumptions are used in the analysis:

- Fluid damping is neglected as there is no water in the AP1000 New Fuel Storage Rack.
- The total effect of  $n$  individual fuel assemblies rattling inside the storage cells in a horizontal plane is modeled as one lumped mass at each of five levels in the fuel rack. Thus, the effect of chaotic fuel mass movement is conservatively ignored.
- For the AP1000 New Fuel Storage Rack, there is no temperature differential and no hot cell.

## **2.5 INPUT DATA**

### **2.5.1 Rack Data**

Table 2-4 contains information regarding the AP1000 New Fuel Storage Rack and fuel data that are used in the analysis. Information is taken from the new fuel rack drawings (Reference 8) (unless noted otherwise).

### **2.5.2 Structural Damping**

Associated with every stiffness element is a damping element with a coefficient consistent with 4% of critical linear viscous damping. This is consistent with the New Fuel design basis Floor Response Spectra set for the AP1000 New Fuel Storage Rack provided in Reference 18 and Reference 21.

### **2.5.3 Material Data**

The necessary material data is shown in Table 2-5. This information is taken from ASME Code Section II, Part D (Reference 13). The values listed correspond to a temperature of 100°F, which is appropriate since new fuel does not release heat.

## **2.6 COMPUTER CODES**

Computer codes used in this analysis are presented in Table 2-15.

## **2.7 ANALYSES**

### **2.7.1 Acceptance Criteria**

The dimensionless stress factors, discussed in subsection 2.3.5, must be less than 1.0. In addition:

- The compressive loads on the cell walls shall be shown to remain below two thirds of the critical buckling load (i.e., a minimum safety factor of 1.5 against buckling is maintained).
- Welds and local stresses must remain below the allowable stress limits corresponding to the material and load conditions, as discussed in greater detail in following sections.

### **2.7.2 Dynamic Simulations**

As discussed earlier, four simulations are performed. The simulations consider the New Fuel Floor Response Spectra and are required to satisfy the stress and kinematic criteria of Reference 6.

## **2.8 RESULTS OF ANALYSES**

The following subsections contain the results obtained from the post-processor DYNAPOST (Reference 15) for the AP1000 New Fuel Storage Rack single-rack analysis under the New Fuel Floor Response Spectra.

## 2.8.1 Time History Simulation Results

Table 2-6 presents the results for major parameters of interest for the new rack for each simulation. Run numbers are as listed in Table 2-2.

### 2.8.1.1 Rack Displacements

The post-processor results summarized in Table 2-7 provide the maximum absolute displacements at the top and bottom corners in the east-west and north-south directions, relative to the pit floor.

### 2.8.1.2 Pedestal Vertical Forces

Run number 1 provides the maximum vertical load on any pedestal. This may be used to assess the structural integrity of the pit floor under the seismic event.

### 2.8.1.3 Pedestal Friction Forces

Run number 3 provides the maximum shear loads; the value is used as an input loading to evaluate the female pedestal-to-baseplate weld (see Table 2-14).

### 2.8.1.4 Impact Loads

The impact loads, such as fuel-to-cell wall and rack-to-wall impacts, are discussed below.

#### Fuel-to-Cell Wall Impact Loads

The maximum fuel-to-cell wall impact load, at any level in the rack, occurs during run number 4.

The most significant load on the fuel assembly arises from rattling during the seismic event. For the five-lumped mass model (with 25% at the 1/4 points and 12.5% at the ends), the limiting lateral load ( $F_e$ ) may be determined as:

$$F_e = \frac{(wxa)}{4} = 27,090 \cdot lbf$$

where:

w = weight of one fuel assembly (conservatively taken to be 1,720 lbs)  
a = permissible lateral acceleration in g's (a=63)

Therefore, a maximum fuel assembly-to-cell wall impact load will yield a safety factor of 13.6.

#### Rack-to-Wall Impacts

The solver summary result files from MR216 (Reference 12) in all of the simulations were manually scanned to determine the maximum impact on each side of the rack. The total rack-to-wall impact at any

one time instant is derived from the output data and calculated for all four simulations. The maximum impact load from the pit walls at the top of the rack is summarized in Table 2-8. The cell region of the AP1000 New Fuel Storage Rack does not impact the pit walls under any of the analyzed conditions.

As discussed in Section 2.2.2.1, the results from the 0.2 coefficient of friction case (run number 1) are not considered credible. Therefore, since the seismic analysis shows no rack-to-wall impacts when run number 1 is ignored, and because the maximum horizontal displacement is less than the specified minimum gap dimension when run number 1 is ignored, the rack-to-wall impacts involving the AP1000 New Fuel Storage Rack are not credible, and the new fuel pit walls are not required to be analyzed for any rack-to-wall impacts.

## **2.8.2 Rack Structural Evaluation**

### **2.8.2.1 Rack Stress Factors**

With time history results available for pedestal normal and lateral interface forces, the limiting bending moment and shear force at the baseplate-to-pedestal interface may be computed as a function of time. In particular, maximum values for the previously defined stress factors can be determined for every pedestal in the AP1000 New Fuel Storage Rack. The maximum stress factor from each simulation is reported in Table 2-6. Using this information, the structural integrity of the pedestal can be assessed. The net section maximum (in time) bending moments and shear forces can also be determined at the bottom of the cellular structure. Based on these, the maximum stress in the limiting rack cell (box) can be evaluated.

Tables 2-6 through 2-13 provide limiting stress factor results for the pedestals in each of the simulations detailed in Table 2-2. The tables also report the stress factors for the AP1000 New Fuel Storage Rack cellular cross section just above the baseplate. These locations are the most heavily loaded net sections in the structure so that satisfaction of the stress factor criteria at these locations ensures that the overall structural criteria set forth in subsection 2.3.3 are met.

The summary of the maximum stress factors for the AP1000 New Fuel Storage Rack for each of the four runs is provided in Table 2-9.

An adjustment factor accounting for the ASME Code slenderness ratio has been calculated. The adjusted factors are identified with \* in the Table 2-9.

All stress factors, as defined in Section 2.3, are less than the mandated limit of 1.0 for the new fuel rack for the governing faulted condition examined. Therefore, the rack is able to maintain its structural integrity under the worst loading conditions.

### **2.8.2.2 Weld Stresses**

Weld locations in the AP1000 New Fuel Storage Rack that are subjected to significant seismic loading are at the bottom of the rack at the baseplate-to-cell connection, at the top of the pedestal support at the baseplate connection, and at the cell-to-cell connections. Bounding values of resultant loads are used to qualify the connections.

## a. Baseplate-to-Rack Cell Welds

Reference 11 (ASME Code Section III, subsection NF) permits, for Level A or B conditions, an allowable weld stress  $\tau = .3 S_u$ . Conservatively assuming that the weld strength is the same as the lower base metal ultimate strength, the allowable stress is given by  $\tau = .3 * (75,000) = 22,500$  psi. As stated in subsection 2.3.4.3, the allowable for Level D is  $0.54 S_u$ , giving an allowable of 40,500 psi.

Weld stresses are determined through the use of a simple conversion (ratio) factor (based on area ratios) applied to the corresponding stress factor in the adjacent rack material. This conversion factor is developed from the differences in base material thickness and length versus weld throat dimension and length:

$$\frac{0.075 * (8.8 + 0.075)}{0.0625 * 0.7071 * 7.0} = 2.1516$$

where:

0.075 is the cell wall thickness  
 8.8+0.075 is the mean box dimension  
 0.0625\*0.7071 is the box-baseplate fillet weld throat size  
 7.0 is the length of the weld

The highest predicted cell to baseplate weld stress is calculated based on the highest R6 value for the rack cell region tension stress factor and R2 and R7 values for the rack cell region shear stress factors (refer to subsection 2.3.5 for definition of these factors). These cell wall stress factors are converted into weld stress values as follows:

$$[R6 * (0.6) + R2 * (0.4) + R7 * (0.4)] * S_y * \text{Ratio} =$$

$$[0.308 * (0.6) + 0.053 * (0.4) + 0.064 * (0.4)] * (25,000) * 2.1516 = 12,458 \text{ psi}$$

The above calculations are conservative for the following reasons:

- 1) The directional stresses associated with the normal stress  $\sigma_y$  and the two shear stresses  $\tau_x$  and  $\tau_y$  should be combined using square root sum of the squares (SRSS) instead of direct summation.
- 2) The maximum stress factors used above do not all occur at the same time instant.

Table 2-10 shows that the weld stresses are acceptable and have safety factors greater than 1.

The corresponding maximum base metal shear stress is shown in Table 2-11.

b. Baseplate-to-Pedestal Welds

The rack weld between baseplate and support pedestal is checked using conservatively imposed loads in a separate finite element model. Table 2-12 summarizes the result.

c. Cell-to-Cell Welds

Cell-to-cell connections are by a series of connecting welds along the cell height. Stresses in storage cell-to-cell welds develop due to fuel assembly impacts with the cell wall. These weld stresses are conservatively calculated by assuming that fuel assemblies in adjacent cells are moving out of phase with one another so that impact loads in two adjacent cells are in opposite directions; this tends to separate the two cells from each other at the weld. The cell-to-cell welds calculation used the maximum stress factor from all of the runs. Both the weld and the base metal shear results are reported in Table 2-13.

### 2.8.2.3 Pedestal Thread Shear Stress

Tables 2-14 provides the limiting thread stress under faulted conditions. The maximum average shear stress in the engagement region occurs in run number 1. This computed stress is applicable to both the male and female pedestal threads.

The allowable shear stress for Level D conditions is the lesser of:  $0.72 S_y = 21,600$  psi or  $0.42 S_u = 31,500$  psi. Therefore, the former criterion controls the allowable shear stress and the limiting result is detailed in Table 2-14.

### 2.8.3 Dead Load Evaluation

The dead load condition is not a governing condition for the AP1000 New Fuel Storage Rack since the general level of loading is far less than the safe shutdown earthquake (SSE) load condition. To illustrate this, it is shown below that the maximum pedestal load is low and that further stress evaluations are unnecessary.

Level A Maximum Pedestal Load	lbf
Dry Weight of 9x8 Rack	24,750
Dry Weight of 72 Intact Fuel Assemblies	140,688
Total Dry Weight	165,438
Load per Pedestal	41,360

This load will induce low stress levels in the neighborhood of the pedestal, compared with the load levels that exist under the SSE load condition (that is, on the order of 270,000 per rack pedestal). Therefore, there are no primary shear loads on the pedestal and since the Level A loads are approximately 1/6 of the Level D loads, while the Level A limits exceed 1/6 of the Level D limits, the SSE load condition bounds the dead load condition and no further evaluation is performed for dead load only.

## 2.8.4 Local Stress Considerations

This subsection presents evaluations for the possibility of cell wall buckling. No secondary stresses due to temperature differences are produced since for the AP1000 New Fuel Storage Rack there is no temperature differential or hot cell.

An ANSYS analysis was performed to evaluate the buckling capacity of the AP1000 New Fuel Storage Rack cells at the base of the rack. The cell wall acts alone in compression for a length of about 6.23 inches up to the point where the neutron absorber sheathing is attached. Above this level the sheathing provides additional strength against buckling; therefore, the analysis focuses on the lower 6.23 inches of the cell wall.

A compressive force equivalent to 9,500 psi is applied to the ANSYS finite element model. It is conservative to use this value since the maximum compressive stress in the outermost cell under seismic loading is:

$$\sigma = (1.2) (25,000) (R6, \text{ which is } 0.308) = 9,240 \text{ psi}$$

The ANSYS analysis demonstrated that the AP1000 New Fuel Storage Rack cells remain in a stable configuration under 1.5 times the maximum seismic load without any gross yielding of the storage cell wall, which satisfies the ASME Code requirements for Level D conditions.

## 2.8.5 Hypothetical Fuel Assembly Drop Accidents

Two fuel assembly drop accident analyses have been performed in accordance with subsection 9.1.1.2.1 C of Reference 1. The objective of the analyses is to assess the extent of permanent damage to the rack:

- 1) A drop of a fuel assembly from 36 inches above the top of the AP1000 New Fuel Storage Rack with subsequent impact on the edge of a cell; and
- 2) A drop of a fuel assembly from 36 inches above the top of the rack straight down through an empty cell with impact on the rack baseplate.

Both analyses are performed using the dynamic simulation code LS-DYNA (Reference 22). A finite element model of one-quarter of the AP1000 New Fuel Storage Rack plus a single fuel assembly is modeled using appropriate shell and solid body elements available in LS-DYNA. The fuel assembly model, which is shown in Figure 2-7, consists of four parts: a rigid bottom end fitting, an elastic beam representing the fuel rods, a lumped mass at the top end of the beam representing the handling tool, and a thin rigid shell that defines the enveloping size and shape of the fuel assembly. The mass and cross-sectional area properties of the elastic beam are based on the entire array of fuel rods (cladding material only). The fuel mass is lumped with the bottom end fitting. Appropriate non-linear material properties have been assigned to the rack components to permit yielding and permanent deformation to occur. Figure 2-8 shows the details of the finite element model in the area where the impacts occur.

For the drop to the top of the AP1000 New Fuel Storage Rack, the fuel assembly is assumed to strike the edge of an exterior cell at a speed corresponding to a 36-inch drop in air and to remain vertical as it is

brought to a stop by the resisting members of the rack. The objective is to demonstrate that the extent of permanent damage to the impacted rack does not extend to the beginning of the active fuel region. For the AP1000 fuel, the top of the active fuel begins approximately 23.27 inches below the top of the rack.

For the drop through an empty cell to the baseplate, the baseplate of the rack is connected to the cells by appropriate welding and a portion of the welding is expected to fail during the impact. The energy from the falling fuel assembly is absorbed by weld failure plus deformation of the baseplate toward the floor. The fuel assemblies surrounding the impacted cell will follow the baseplate deformation and the objective is to determine how many fuel assemblies displace an amount sufficient to bring their active fuel region below the limit of the absorbing material attached to each fuel cell wall. In the case of the AP1000 New Fuel Storage Rack, a 2-inch vertical movement of a fuel assembly, relative to the cell wall, does not require any new criticality evaluation.

The results from the analyses are shown in Figures 2-9 and 2-10. For the drop to the top of the AP1000 New Fuel Storage Rack, the extent of permanent damage is limited to a depth of 12.75 inches. The tops of the poison panels are located 21.27 inches below the top of the rack. The poison panels overlap the active fuel by two inches at the top and bottom. The top of the active fuel begins approximately 23.27 inches below the top of the rack, therefore, the active fuel region remains surrounded by an undamaged cell wall and no further criticality evaluation is required.

For the drop to the baseplate of the rack, Figure 2-10 shows that only the dropped fuel assembly is moved downward more than 2 inches and exposes active fuel on all four sides. An additional 8 fuel assemblies may drop a sufficient distance to expose active fuel on two or three sides. The consequences to reactivity of this event are discussed in subsection 2.4.2 of Reference 4.

### **2.8.6 Stuck Fuel Assembly Evaluation**

A nearly empty rack with one corner cell occupied is subject to an upward load of 4,000 lbf, which is assumed to be caused by the fuel sticking while being removed. The ramification of the loading is two-fold:

1. The upward load creates a force and a moment at the base of the rack;
2. The loading induces a local tension in the cell wall and shear stresses in the adjacent welds.

Strength of materials calculations have been performed to determine the maximum stress in the rack cell structure due to a postulated stuck fuel assembly. The results are summarized in Table 2-17.

## **2.9 CONCLUSIONS**

From the results of the single-rack analyses, the following conclusions are made regarding the design and layout of the AP1000 New Fuel Storage Rack.

- All rack cell wall and pedestal stress factors are below the allowable stress factor limit of 1.0.

- The compressive loads on the rack cellular structure during a seismic event are less than two thirds the critical buckling load.
- All weld stresses are below the allowable limits.
- There are no rack-to-wall impacts under realistic pit conditions (i.e., when the coefficient of friction is greater than or equal to 0.5).
- A stuck fuel assembly results in stress conditions within the allowable limits.
- Two fuel assembly drops were analyzed. The drop on to the New Fuel Rack Storage does not require a criticality evaluation. The drop of a fuel assembly straight through an empty cell has been evaluated in Reference 4 and was found acceptable.

It is therefore considered demonstrated that the design of the AP1000 New Fuel Storage Rack meets the requirements for structural integrity for the postulated Level A and Level D conditions defined.

<b>Parameter</b>	<b>Nominal Dimension (in) or Material</b>
Cell Pitch	10.9
Cell ID	8.8
Cell Length	199.5
Cell Wall Thickness	0.075
Cell Wall Material	SS-304
Metamic Width	7.5
Metamic Thickness	0.106
Metamic Composition	B <sub>4</sub> C/Al
Sheathing Thickness	0.035
Sheathing Material	SS-304

<b>Coefficient of Friction</b>	<b>Loading Configuration</b>	<b>Seismic Input (Floor Response Spectra)</b>	<b>Run Number</b>
0.2	Fully Loaded	New Fuel	1
0.5	Fully Loaded	New Fuel	2
0.8	Fully Loaded	New Fuel	3
0.8	Partially Loaded <sup>(1)</sup>	New Fuel	4

**Note:**

- See Figure 2-11 for the partially loaded layout configuration.

<b>Table 2-3 Loading Combinations for AP1000 New Fuel Storage Rack</b>	
<b>Loading Combination</b>	<b>Service Level</b>
D + L D + L + T <sub>o</sub>	Level A
D + L + T <sub>a</sub> D + L + T <sub>o</sub> + P <sub>f</sub>	Level B
D + L + T <sub>a</sub> + E'	Level D
D + L + F <sub>d</sub>	The functional capability of the fuel rack should be demonstrated.
<p><b>Notes:</b></p> <ol style="list-style-type: none"> <li>There is no operating basis earthquake (OBE) for the AP1000 plant.</li> <li>The AP1000 New Fuel Storage Rack is freestanding; thus, there is minimal or no restraint against free thermal expansion at the base of the rack. As a result, thermal loads applied to the rack (T<sub>o</sub> and T<sub>a</sub>) produce only local (secondary) stresses.</li> </ol> <p>Abbreviations are those used in Reference 6:</p> <p>D = Dead weight induced loads (including fuel assembly weight)</p> <p>L = Live load (not applicable to fuel racks since there are no moving objects in the rack load path)</p> <p>F<sub>d</sub> = Force caused by the accidental drop of the heaviest load from the maximum possible height</p> <p>P<sub>f</sub> = Upward force on the rack caused by postulated stuck fuel assembly</p> <p>E' = Safe Shutdown Earthquake (SSE)</p> <p>T<sub>o</sub> = Differential temperature induced loads based on the most critical transient or steady state condition under normal operation or shutdown conditions</p> <p>T<sub>a</sub> = Differential temperature induced loads based on the postulated abnormal design conditions</p>	

<b>Table 2-4 AP1000 New Fuel Storage Rack and Fuel Data</b>		
<b>Geometric Parameter</b>		<b>Dimension (in) Unless Noted</b>
<b>Composite Box Data</b>		
Box ID		8.8
Pitch		10.9
Wall Thickness		0.075
<b>Rack Module Data</b>		
Cell Length		199.5
Support Height		2.75
Female Pedestal Side Dim		11.0 x 11.0 square
Female Pedestal Height		2.25
Male Pedestal Diameter		4.5
Total Height		204.5
Baseplate Thickness		0.75
Baseplate Extension		1.0
<b>Fuel Data</b>		
Minimum Dry Fuel Weight (excluding Control Components) (lb)		1,720 (Reference 19)
Maximum Dry Fuel Weight (including Control Components) (lb)		1,954 (Reference 19)
Maximum Nominal Fuel Assembly Size		8.404 (Reference 19)
Minimum Nominal Fuel Assembly Size		8.246 (Reference 19)
<b>Rack Details</b>		
<b>Rack</b>	<b>Array Size</b>	<b>Weight (lb)</b>
New Fuel Rack	9 x 8	24,750

<b>Table 2-5 Material Data (ASME - Section II, Part D)</b>			
<b>Material</b>	<b>Young's Modulus E (psi)</b>	<b>Yield Strength S<sub>y</sub> (psi)</b>	<b>Ultimate Strength S<sub>u</sub> (psi)</b>
<b>Rack Material Data (100°F)</b>			
SA-240, Type 304	27.9 x 10 <sup>6</sup>	30,000	75,000
<b>Support Material Data (100°F)</b>			
SA-240, Type 304 (Upper part of support feet)	27.9 x 10 <sup>6</sup>	30,000	75,000
SA-564, Type 630 (Hardened at 1100° F)	27.9 x 10 <sup>6</sup>	115,000	140,000

<b>Table 2-6 Results Summary</b>					
<b>Coefficient of Friction</b>	<b>Run No.</b>	<b>Max. Stress Factor</b>	<b>Max. Vertical Load (lbf)</b>	<b>Max. Shear Load (lbf) (X or Y)</b>	<b>Max. Fuel-to-Cell Wall Impact (lbf)</b>
0.2	1	0.302	270,000	48,350	1,133
0.5	2	0.302	263,000	88,400	1,167
0.8	3	0.308	263,000	147,000	1,722
0.8	4	0.177	162,000	95,400	1,992

<b>Table 2-7 Time History Post-Processor Results</b>		
<b>Location on Rack</b>	<b>Maximum Rack Displacement Relative to Floor (in)</b>	<b>Run Number</b>
Base Plate (North-South)	5.95	1
Top of Rack (North-South)	6.35	1
Base Plate (East-West)	2.78	1
Top of Rack (East-West)	3.65	1

<b>Table 2-8 Rack-to-Wall Impacts</b>		
<b>Coefficient of Friction</b>	<b>Maximum Rack-to-Wall Impact Load on One Side of Rack (lbf)</b>	<b>Run Number</b>
0.2	154,600	1

Coefficient of Friction	Pedestal Stress Factor	Cell Wall Stress Factor	Run Number
0.2	0.110	0.302 $\left(0.302 \times \left(\frac{1}{0.773}\right)\right) = 0.390^*$	1
0.5	0.108	0.302 $\left(0.302 \times \left(\frac{1}{0.773}\right)\right) = 0.390^*$	2
0.8	0.124	0.308 $\left(0.308 \times \left(\frac{1}{0.773}\right)\right) = 0.398^*$	3
0.8	0.098	0.177 $\left(0.177 \times \left(\frac{1}{0.773}\right)\right) = 0.229^*$	4

**Note:**  
\* Adjustment factor accounting for ASME Code Slenderness Ratio

Weld Stress (psi)	Allowable Stress (psi)	Safety Factor
12,458	40,500	3.25

Base Metal Shear Stress (psi)	Allowable Stress (psi)	Safety Factor
8,807	21,600	2.45

Weld Stress (psi)	Run No.	Allowable Stress (psi)	Safety Factor
13,360	3	40,500	3.03

**Table 2-13 Weld and Base Metal Shear Results**

<b>Analysis Type</b>	<b>Stress (psi)</b>	<b>Run No.</b>	<b>Allowable Stress (psi)</b>	<b>Safety Factor</b>
Weld	17,787	4	40,500	2.28
Base Metal Shear	12,577	4	21,600	1.72

**Table 2-14 Pedestal Thread Shear Stress**

<b>Base Metal Shear Stress (psi)</b>	<b>Allowable Stress (psi)</b>	<b>Safety Factor</b>
19,149	21,600	1.128

<b>Code</b>	<b>Version</b>	<b>Description</b>
GENEQ	1.3	Generates artificial time histories from input response spectra set.
CORRE	1.3	Uses results from GENEQ and demonstrates required statistical independence of time histories.
PSD1	1.0	Uses results from GENEQ and compares regenerated Power Spectral Densities with target.
WORKING MODEL	2004	Is a Rigid Body Dynamics code used to improve baseline correction.
VMCHANGE	4.0	For a dry pool, develops a zero matrix of size = (number of racks x 22 DOF per rack).
MULTI1	1.55	Incorporates appropriate non-zero values due to structural effects that are put in appropriate locations in the output matrix from VMCHANGE to form the final mass matrix for the analysis. The appropriate non-zero right-hand sides are also developed.
MASSINV	2.1	Calculates the inverse of the mass matrix.
MSREFINE	2.1	Refines the inverse of the mass matrix.
PREDYNA1	1.5	Generates various input lines for the input file required to run the dynamic solver.
PD16	2.1	Generates rack-to-fuel compression-only impact springs, rack-to-ground impact springs, and rack elastic deflection springs for each rack being analyzed and creates the appropriate lines of input for the solver.
SPG16	3.0	Generates compression-only rack-to-rack impact springs for the specific rack configuration in the pool for the solver.
MR216	2.0	Is a solver for the dynamic analysis of the racks; uses an input file from the cumulative output from PREDYNA, PD16, and SPG16, together with the mass matrix, right-hand side matrix, and the final time histories from GENEQ.
DYNAPOST	2.0	Post-Processor for MR216; generates safety factors, maximum pedestal forces, and maximum rack movements.
ANSYS	9.0	Is a general purpose commercial FEA code.
LS-DYNA	970	General purpose commercial FEA code optimized for shock and impact analyses

<b>Table 2-16 Degrees of Freedom for Single Rack Dynamic Model</b>						
<u>Location (Node)</u>	<u>Displacement</u>			<u>Rotation</u>		
	$U_x$	$U_y$	$U_z$	$\theta_x$	$\theta_y$	$\theta_z$
1	$p_1$	$p_2$	$p_3$	$q_4$	$q_5$	$q_6$
2	$p_7$	$p_8$	$p_9$	$q_{10}$	$q_{11}$	$q_{12}$
Node 1 is assumed to be attached to the rack at the bottom most point. Node 2 is assumed to be attached to the rack at the top most point. Refer to Figure 2-2 for node identification.						
2*	$p_{13}$	$p_{14}$				
3*	$p_{15}$	$p_{16}$				
4*	$p_{17}$	$p_{18}$				
5*	$p_{19}$	$p_{20}$				
1*	$p_{21}$	$p_{22}$				
<p>where the relative displacement variables <math>q_i</math> are defined as:</p> <p><math>p_i = q_i(t) + U_x(t)</math> <math>i = 1, 7, 13, 15, 17, 19, 21</math>  <math>= q_i(t) + U_y(t)</math> <math>i = 2, 8, 14, 16, 18, 20, 22</math>  <math>= q_i(t) + U_z(t)</math> <math>i = 3, 9</math>  <math>= q_i(t)</math> <math>i = 4, 5, 6, 10, 11, 12</math></p> <p><math>p_i</math> denotes absolute displacement (or rotation) with respect to inertial space  <math>q_i</math> denotes relative displacement (or rotation) with respect to the floor slab</p> <p>* denotes fuel mass nodes  <math>U(t)</math> are the three known earthquake displacements</p>						

<b>Table 2-17 Results from Stuck Fuel Assembly Evaluation</b>			
<b>Item</b>	<b>Calculated Stress (psi)</b>	<b>Allowable Stress (psi)</b>	<b>Safety Factor</b>
Tensile Stress in Cell Wall	4,046	18,000	4.45
Shear Stress in Cell-to-Cell Weld	15,085	22,500	1.49

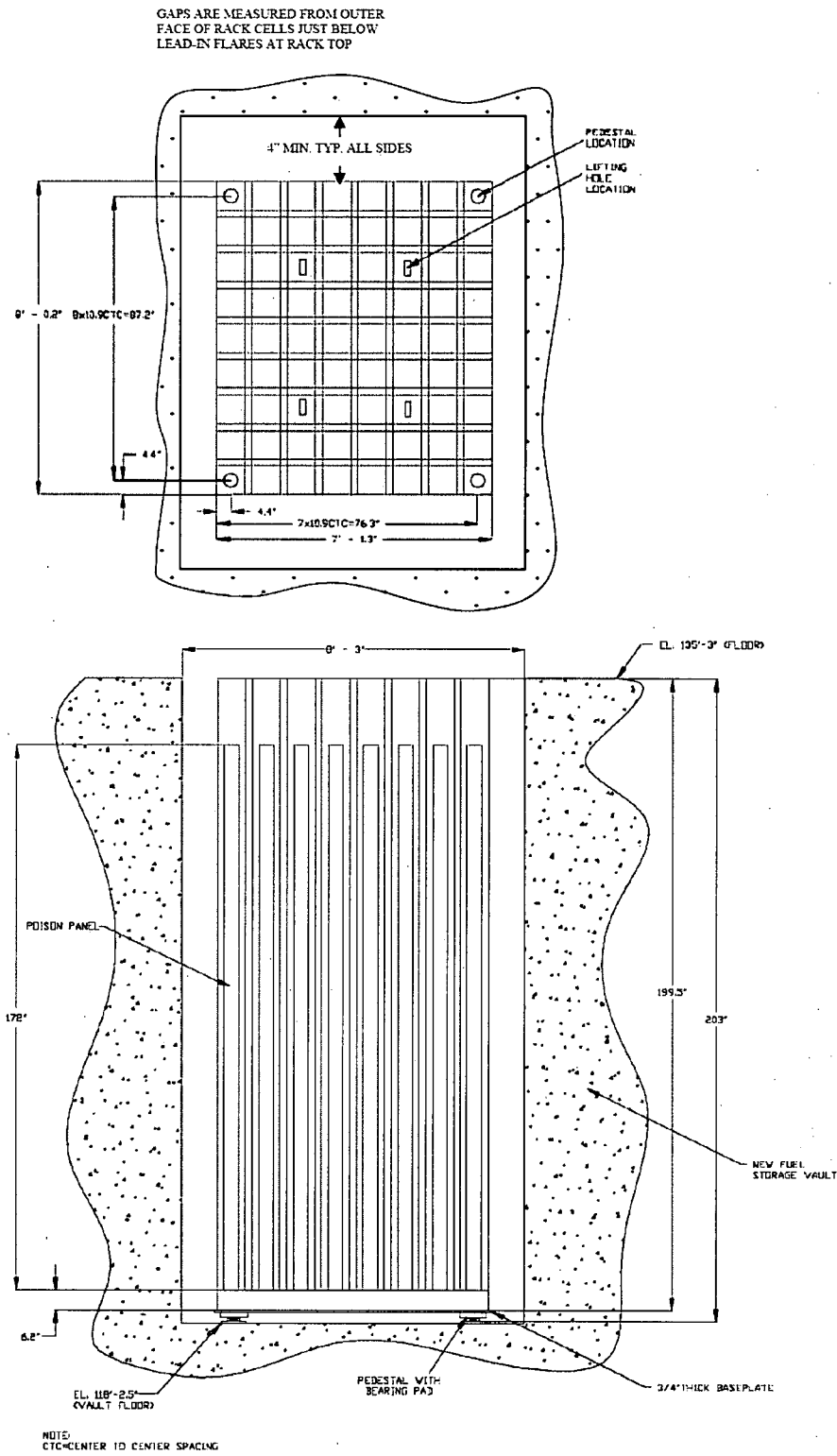


Figure 2-1 Configuration of New Fuel Storage Rack (Sheet 1 of 2)

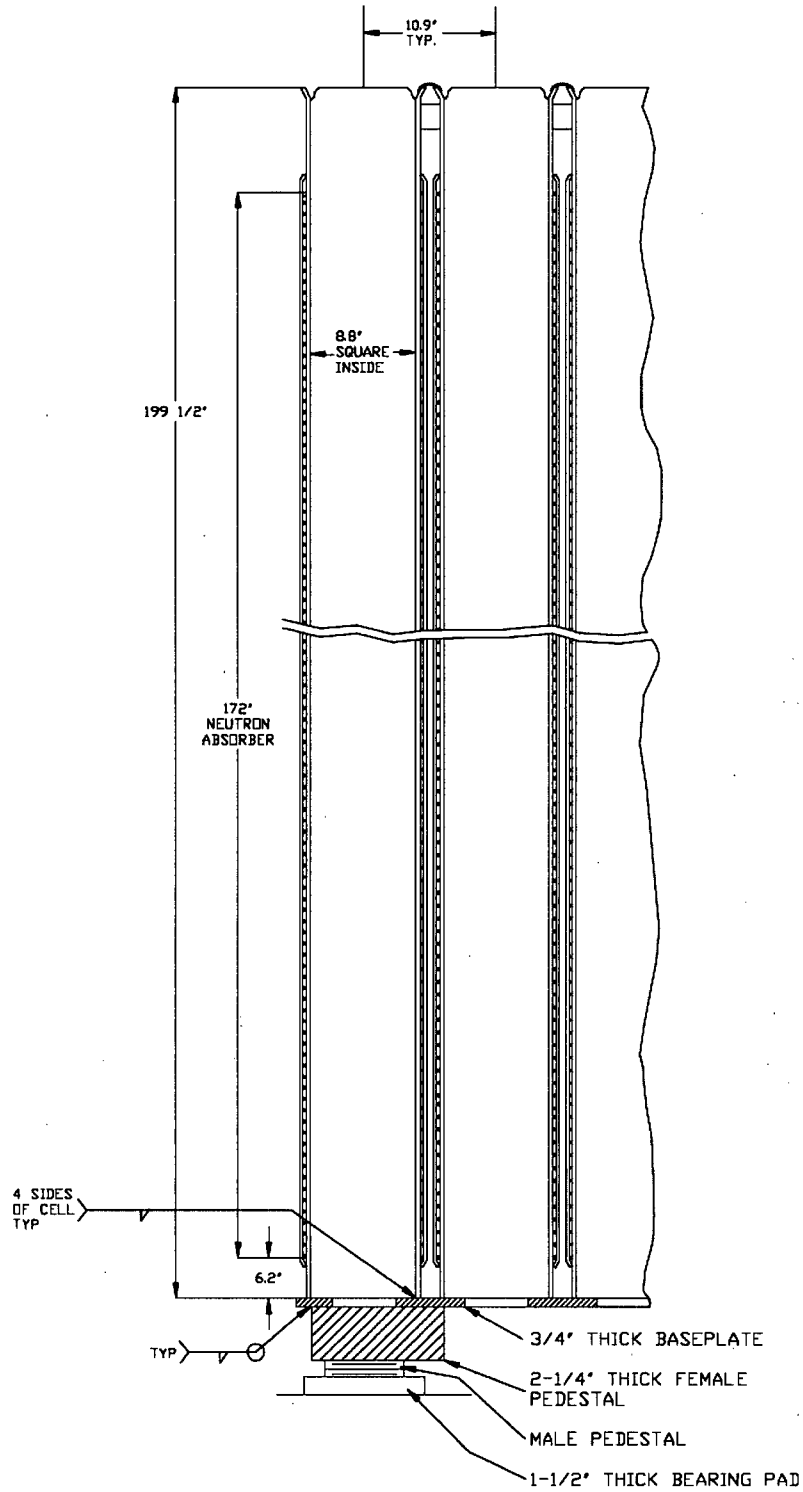


Figure 2-1 Configuration of New Fuel Storage Rack (Sheet 2 of 2)

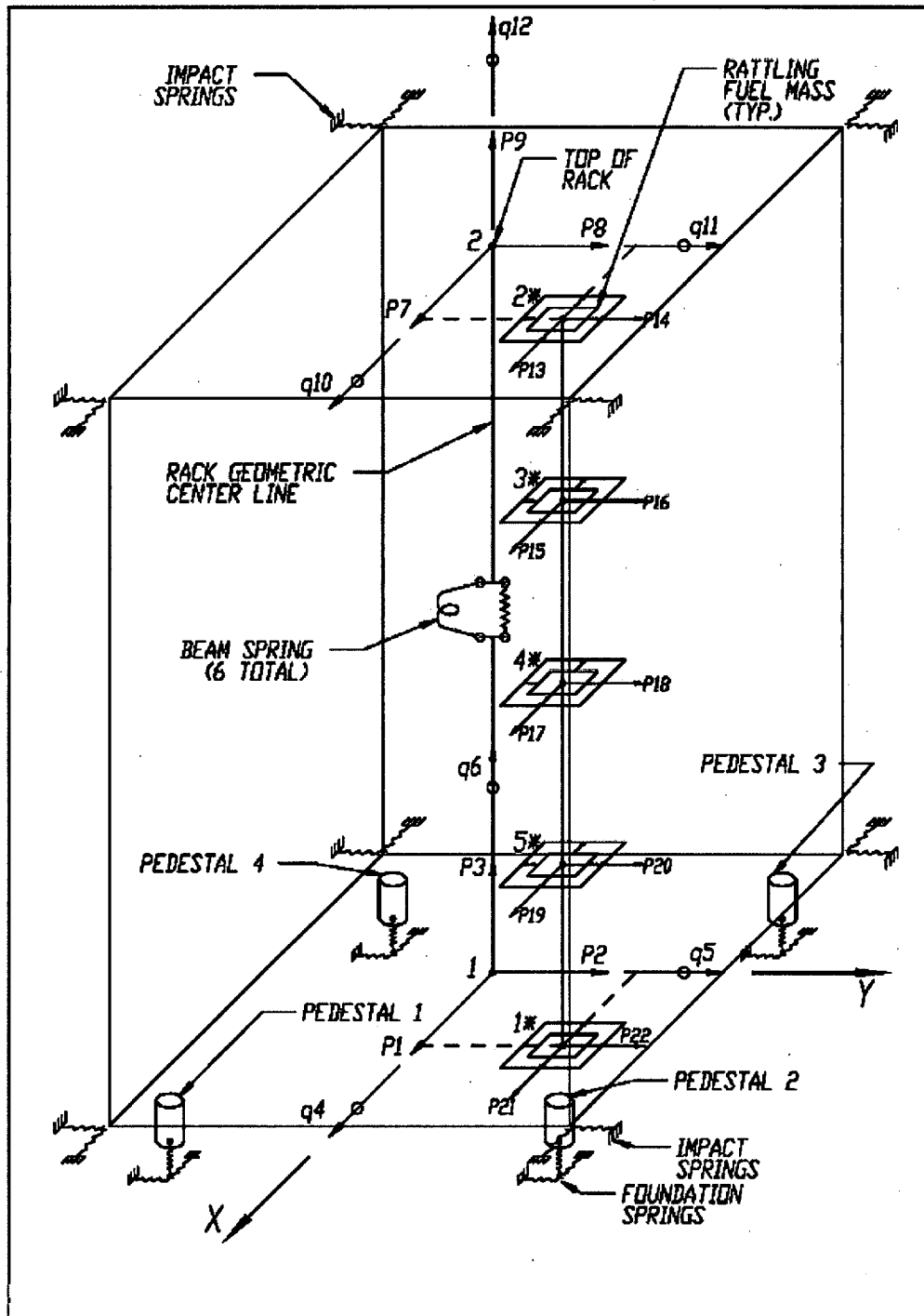


Figure 2-2 Schematic Diagram of Dynamic Model for DYNARACK

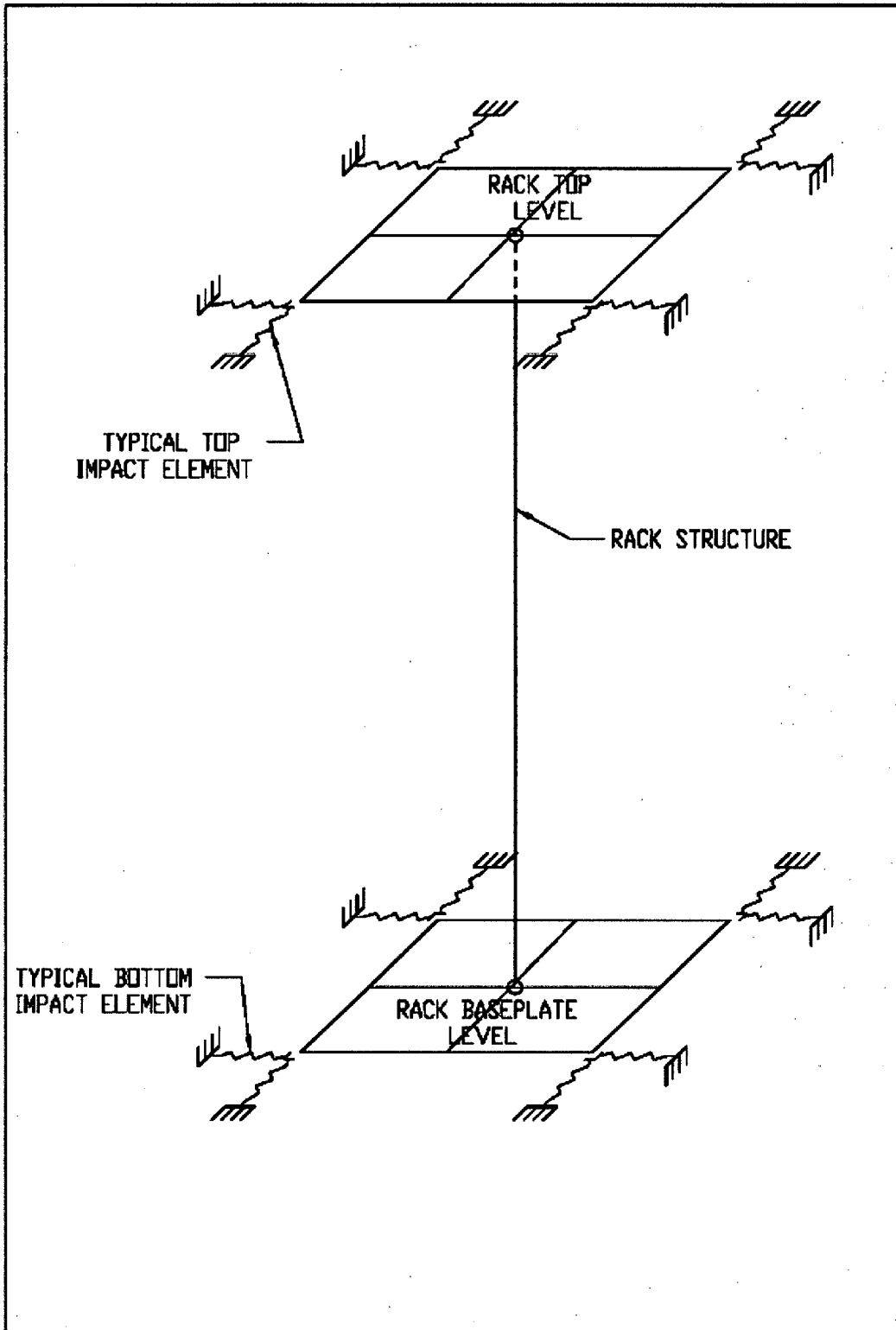


Figure 2-3 Rack-to-Rack Impact Springs

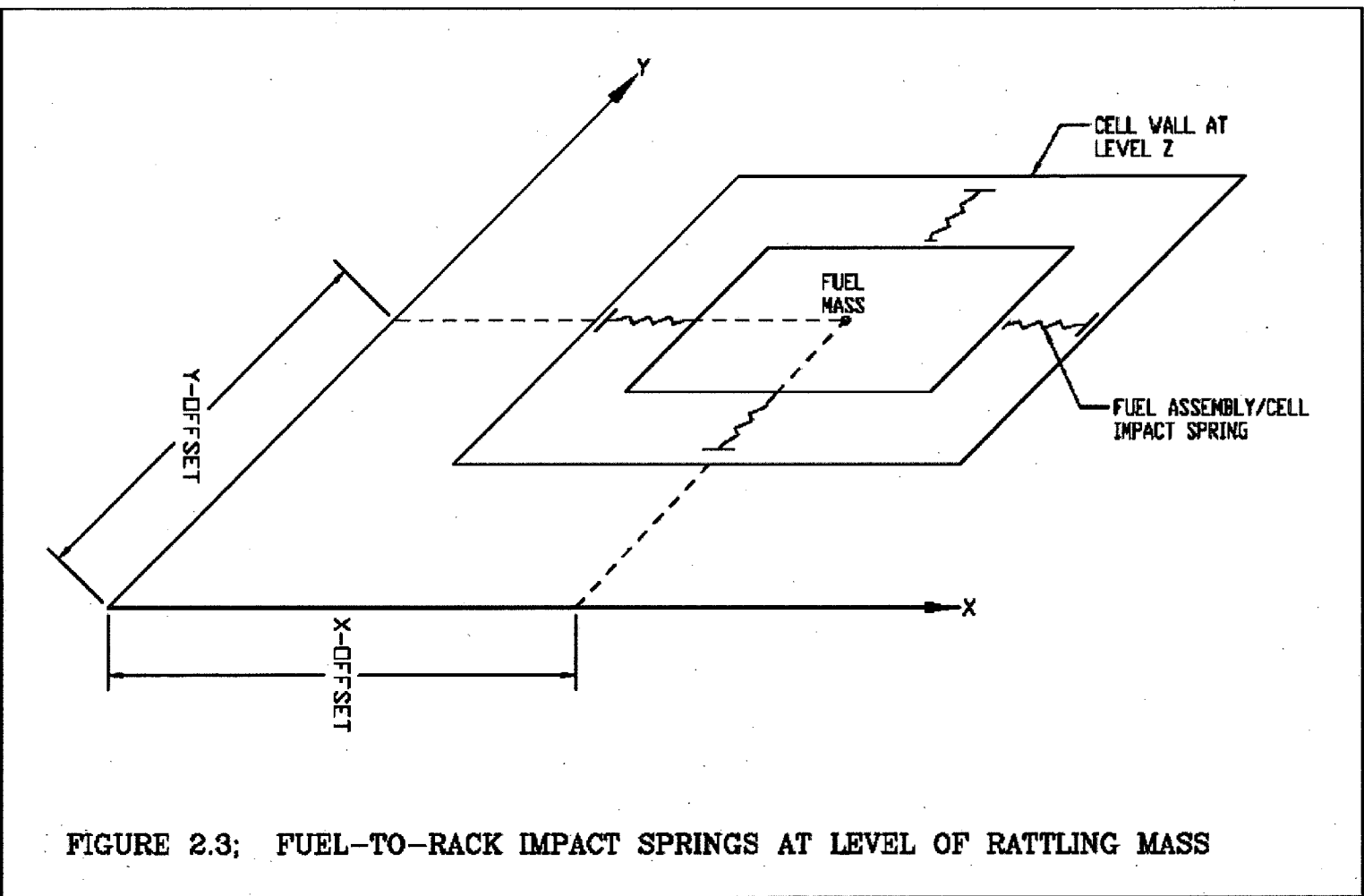


Figure 2-4 Fuel-to-Rack Impact Springs at Level of Rattling Mass

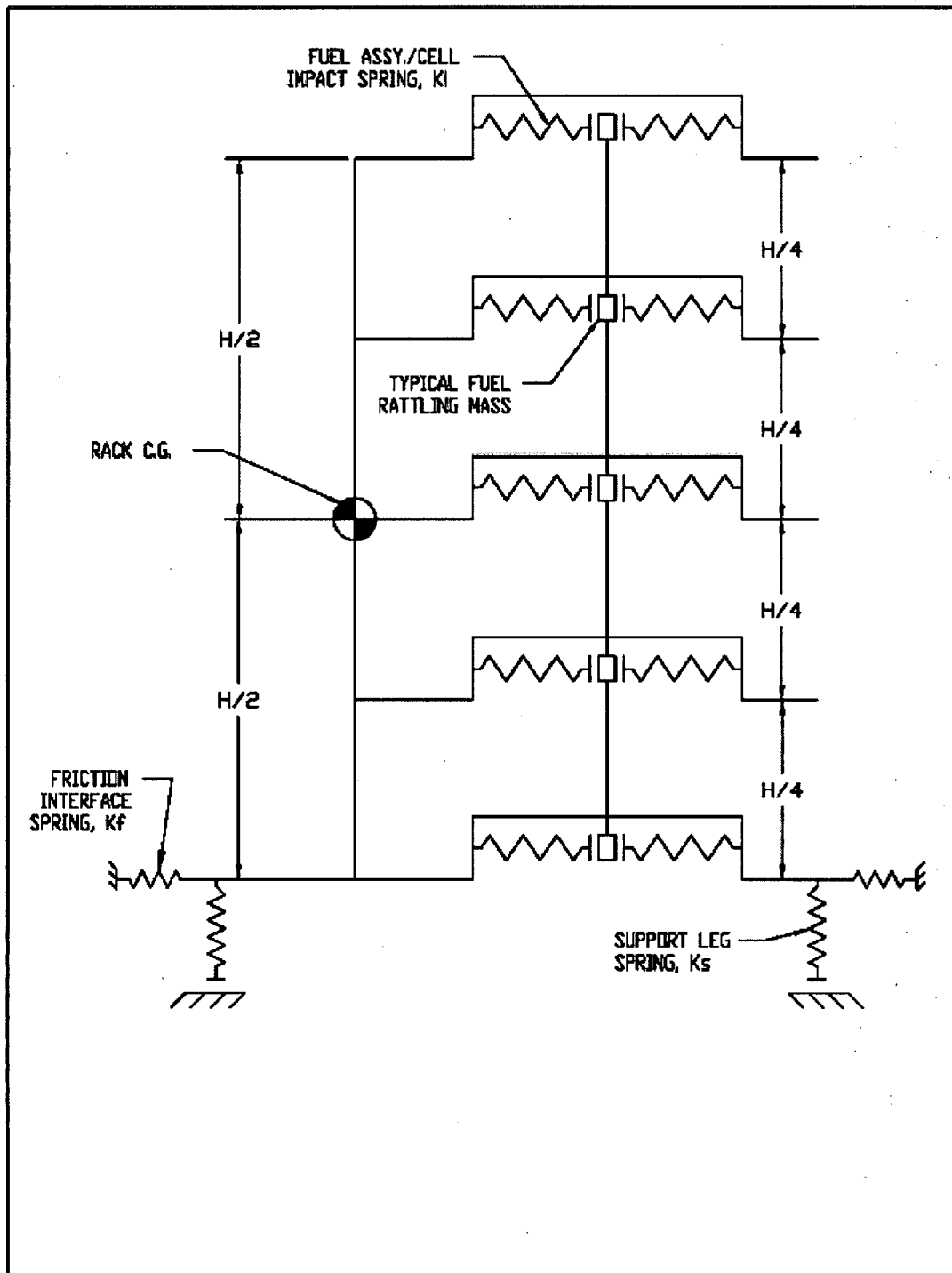
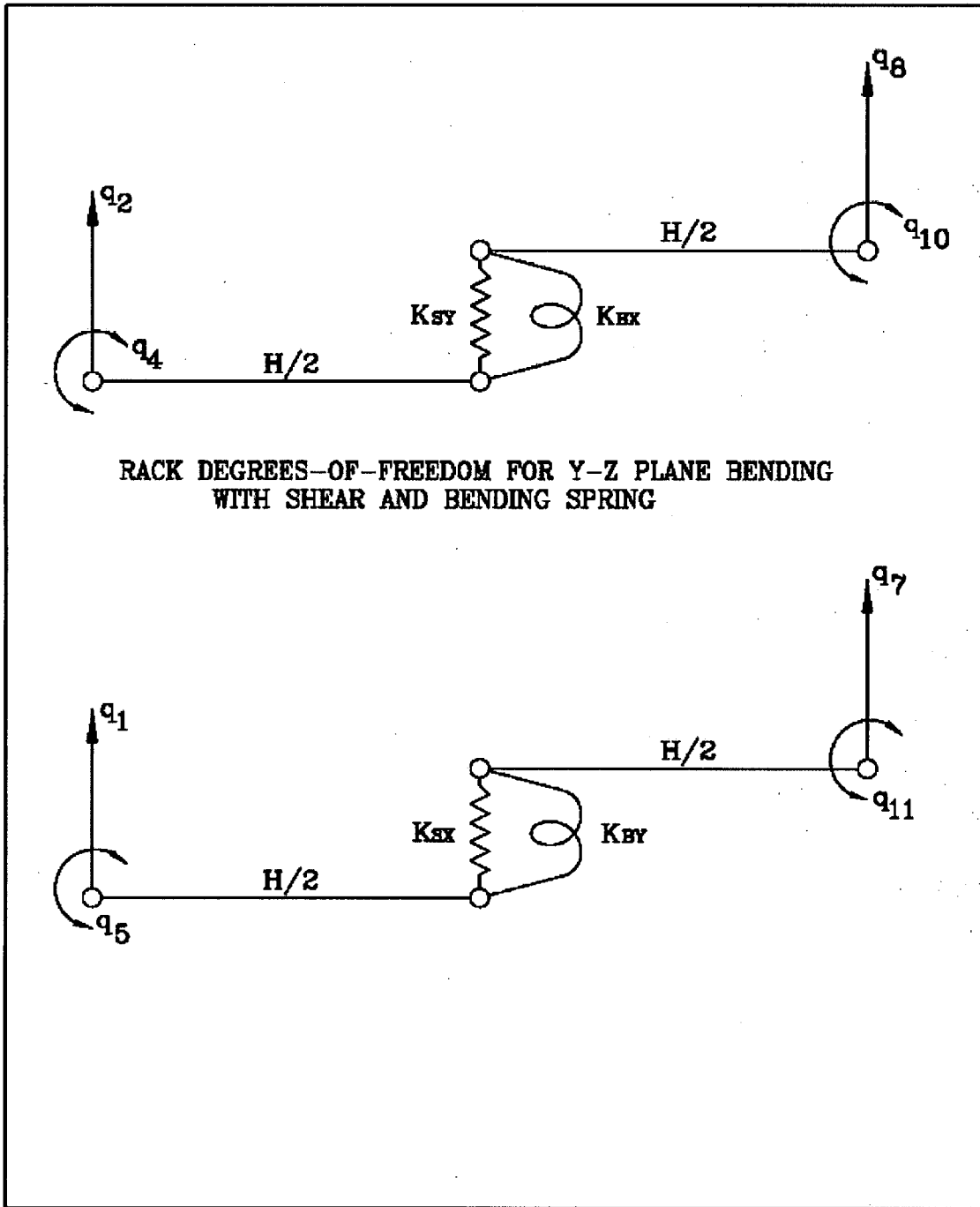


Figure 2-5 Two-Dimensional View of Spring-Mass Simulation



**Figure 2-6 Rack Degrees-of-Freedom for X-Y Plane Bending with Shear and Bending Spring**

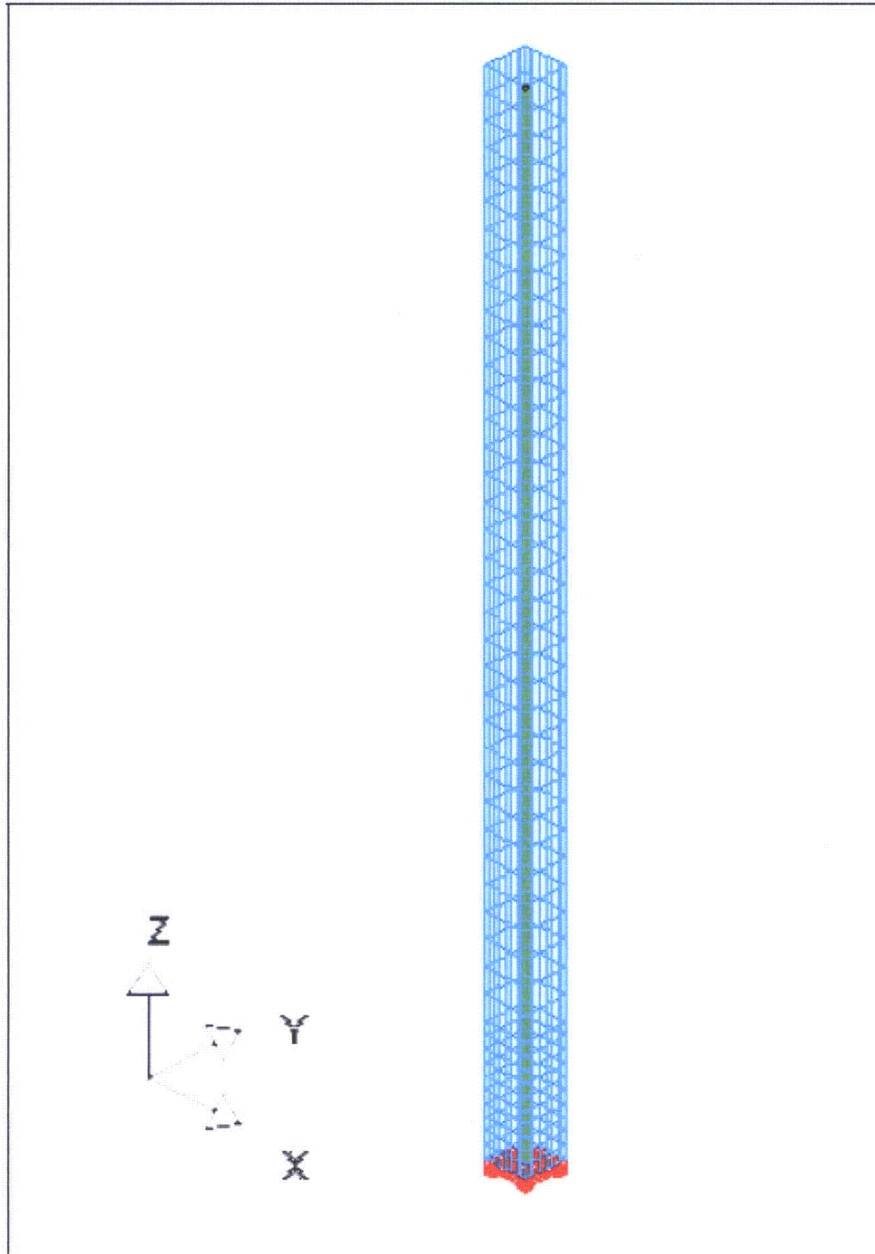


Figure 2-7 LS-DYNA Model of Dropped Fuel Assembly

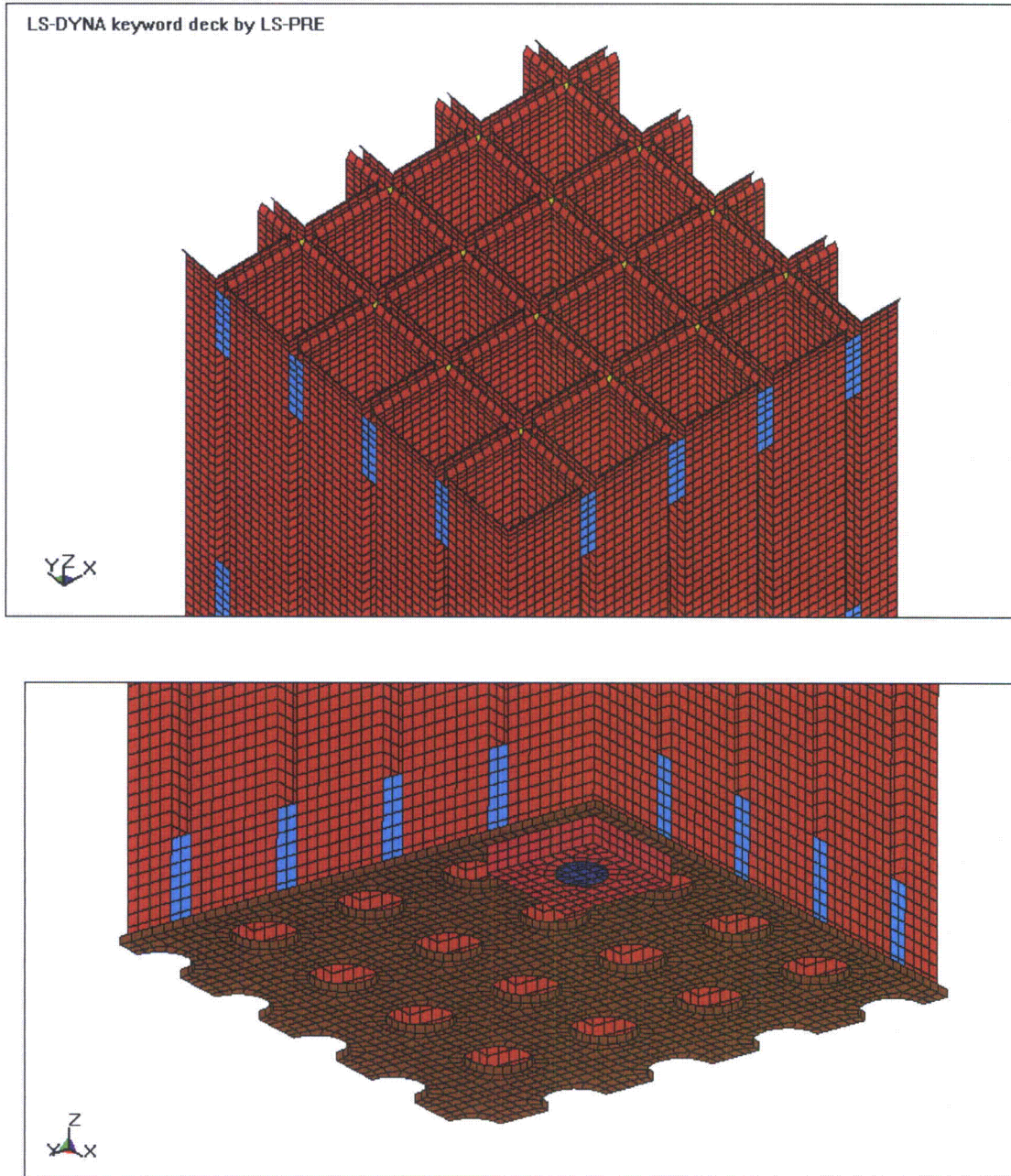


Figure 2-8 LS-DYNA Model of Top and Bottom of AP1000 New Fuel Storage Rack

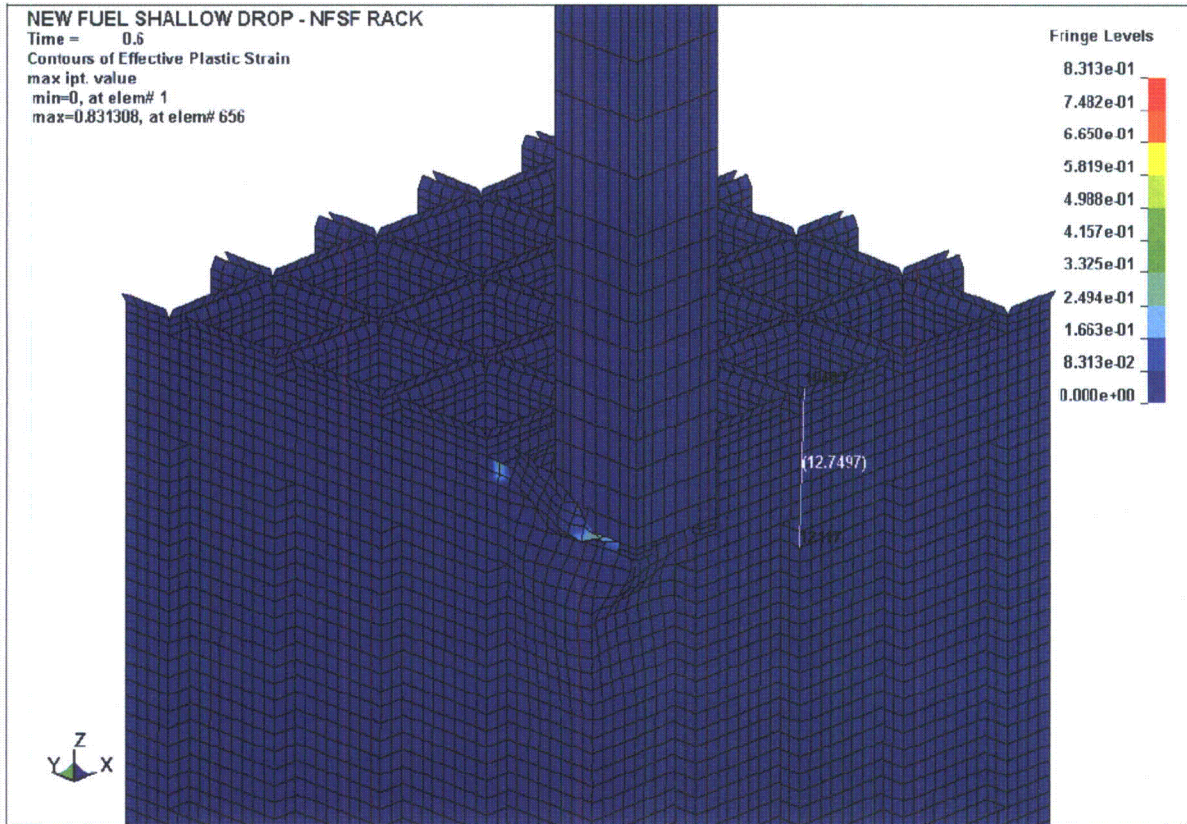
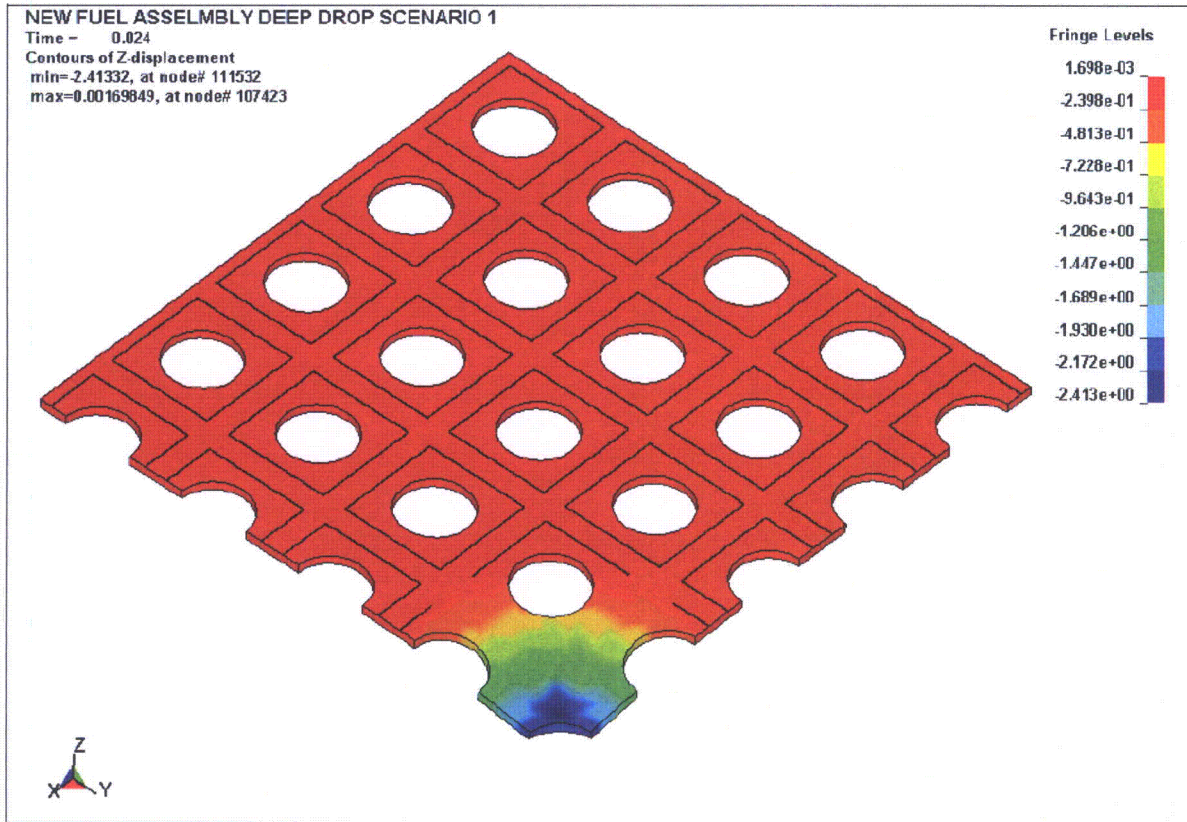


Figure 2-9 Results from Drop on AP1000 New Fuel Storage Rack



**Figure 2-10 Baseplate Deformation Resulting from Fuel Assembly Drop onto Baseplate (2.41 inch Maximum Displacement Directly under Impact Location)**

### 3 REGULATORY IMPACT

The structure/seismic analysis of the AP1000 New Fuel Storage Rack is addressed in subsection 9.1.1.2.1, "New Fuel Rack Design," of the NRC Final Safety Evaluation Report (Reference 2). The completion of the structural/seismic analysis for the AP1000 New Fuel Storage Rack is identified in the Final Safety Evaluation Report as COL Action Item 9.1.6-1.

The changes to the DCD presented in Revisions 0 and 1 of this report do not represent an adverse change to the design functions of the AP1000 New Fuel Storage Rack, or to how design functions are performed or controlled. The structural/seismic analysis of the AP1000 New Fuel Storage Rack is consistent with the description of the analysis in subsection 9.1.1.2.1, "New Fuel Rack Design," of the DCD. Therefore, the changes to the DCD do not involve revising or replacing a DCD-described evaluation methodology. The changes to the DCD do not involve a test or experiment not described in the DCD. The DCD change does not require a license amendment per the criteria of VIII.B.5.b. of Appendix D to 10 CFR Part 52.

None of the changes described involve design features used to mitigate severe accidents. Therefore, a license amendment based on the criteria of VIII.B.5.c of Appendix D to 10 CFR Part 52 is not required.

The closure of the COL Information Item will not alter barriers or alarms that control access to protected areas of the plant. The closure of the COL Information Item will not alter requirements for security personnel. Therefore, the closure of the COL Information Item does not have an adverse impact on the security assessment of the AP1000.

## 4 REFERENCES

1. APP-GW-GL-700, AP1000 Design Control Document, Revision 17.
2. Final Safety Evaluation Report Related to Certification of the AP1000 Standard Design, September 2004.
3. Westinghouse Calculation: APP-FS01-S3C-001, Rev. 2, "AP1000 New Fuel Storage Rack Structural/Seismic Analysis," November 2009. (Westinghouse Proprietary)
4. AP1000 Standard Combined License Technical Report, APP-GW-GLR-030, Rev. 0, "New Fuel Storage Rack Design Criticality Analysis," May 2006.
5. Deleted.
6. U.S. NRC Standard Review Plan, NUREG-0800 (SRP 3.8.4, Rev. 1).
7. U.S. NRC Standard Review Plan, NUREG-0800 (SRP 3.7.1, Rev. 2).
8. Westinghouse Documents: APP-FS01-V1-003, APP-FS01-V2-002, and APP-FS01-V6-006, "New Fuel Storage Rack Layout," all Rev. 2. (Westinghouse Proprietary)
9. Soler, A.I. and Singh, K.P., "Seismic Responses of Free Standing Fuel Rack Constructions to 3-D Motions," Nuclear Engineering and Design, Vol. 80, pp. 315-329 (1984).
10. Levy, S., and Wilkinson, John, "The Component Element Method in Dynamics," McGraw Hill, 1976.
11. ASME Boiler & Pressure Vessel Code Section III, Subsection NF, 1998 Edition with 2000 Addenda.
12. Holtec Computer Code MR216 (multi-rack transient analysis code, a.k.a. DYNARACK), Version 2.00. QA documentation contained in Holtec Report HI-92844. (Holtec Proprietary)
13. ASME Boiler & Pressure Vessel Code, Section II, Part D, 1998 Edition with 2000 Addenda.
14. ASME Boiler & Pressure Vessel Code, Section III, Appendices, 1998 Edition with 2000 Addenda.
15. Holtec Computer Code DYNAPOST (Analysis Post Processor), v. 2.0. (Holtec Proprietary)
16. RORARK'S Formulas for Stress & Strain, 6<sup>th</sup> edition, Warren C. Young, McGraw Hill.
17. Deleted.

18. AP1000 Letter Number DCP/HII0012, "Input Spectra for Revised Fuel Rack Analyses", from J.M. Iacovino (Westinghouse Electric Company) to Mr. Evan Rosenbaum (Holtec International), Dated October 18, 2007. (Westinghouse Proprietary)
19. Westinghouse Document: APP-RXS-M8-020, Rev. 1, "AP1000 NSSS / Core Design Interface Document", March 2009. (Westinghouse Proprietary)
20. Rabinowicz, E., "Friction Coefficients of Water Lubricated Stainless Steels for a Spent Fuel Rack Facility," MIT, a report for Boston Edison Company, 1976.
21. Westinghouse Document: APP-GW-G1-003, Rev. 3, "AP1000 Seismic Design Criteria," May 2009. (Westinghouse Proprietary)
22. LS-DYNA, v. 970 Livermore Software Technology Corporation, 2005.
23. Deleted.
24. Westinghouse Calculation: APP-GW-S2R-010, Rev. 3, "Extension of Nuclear Island Analysis to Soil Sites," November 2008. (Westinghouse Proprietary)
25. U.S. NRC Standard Review Plan NUREG-0800 (SRP 3.8.4, Rev. 2).
26. U.S. NRC, Regulatory Guide 1.124, Rev. 1, "Service Limits and Loading Combinations for Class 1 Linear-Type Component Supports," January 1978.
27. U.S. NRC, Regulatory Guide 1.124, Rev. 2, "Service Limits and Loading Combinations for Class 1 Linear-Type Component Supports," February 2007.
28. Westinghouse Calculation: APP-FS02-Z0C-001, Rev. 2, "Analyses of AP1000 Fuel Storage Racks Subjected to Fuel Drop Accidents", July 2009. (Westinghouse Proprietary)
29. "Marks' Standard Handbook for Mechanical Engineers", 10<sup>th</sup> Edition, Theodore Baumeister, 1996.

## 5 DCD MARKUP

There are no DCD changes as a result of Revision 2 of APP-GW-GLR-026. All DCD markups were detailed in the RAIs that were the basis for this revision. The following RAI responses included a DCD markup: RAI-SRP9.1.2-SEB1-01 (Revision 1), RAI-TR44-016 (Revision 2) and RAI-TR44-017 (Revision 2). The changes identified in those responses will be incorporated into a future revision of the DCD.